



# THE UNIVERSITY OF QUEENSLAND

## Bachelor of Engineering Thesis

### Unmanned Aerial Vehicle Implementation in Renewable Energy Applications

Student Name: Edward GREENAWAY

Course Code: MECH4500

Supervisor: Dr Andras Nagy

Submission date: 28 October 2016

A thesis submitted in partial fulfilment of the requirements of the  
Bachelor of Engineering degree  
in Mechanical & Aerospace Engineering

UQ Engineering

Faculty of Engineering, Architecture and Information Technology

# Contents

Acknowledgements.....	3
Abstract .....	4
1.0 Introduction .....	5
2.0 Background.....	7
2.1 Concentrated Solar Power.....	7
2.2 Wind Power .....	10
2.3 Power Plant Cooling Towers.....	12
2.4 Comparisons .....	14
3.0 Unmanned Aerial Vehicle.....	17
3.1 Unmanned Aerial Vehicle Literature .....	17
3.2 Selection Criteria and Considered Vehicles .....	20
3.3 Recommendation.....	22
4.0 Implementation of the Vehicle .....	23
4.1 Sensors .....	23
4.2 Operational Scenario .....	25
4.3 Enabling Technologies .....	28
4.4 Upgradability.....	30
5.0 Conclusion .....	37
6.0 References.....	38
Appendices.....	44
Appendix A.....	44
Appendix B.....	45

## Acknowledgements

*I'd like to acknowledge the assistance of several people throughout this thesis. Firstly, my supervisor, Andras Nagy, who has always been happy and relaxed as he provided guidance. Secondly I'd like to thank Byron Burgess-Gallop, whose cooperation and eagerness to assist with the development of our linked projects was greatly appreciated. Thirdly, my friends and family, you know who you are. A special mention goes to Marguerite Taylor, for always being there throughout my university studies. Finally, I'd like to thank my legs for always supporting me, my arms for always being by my side, and my hands for always being within arm's reach.*

## Abstract

The possibility of implementing an Unmanned Aerial Vehicle (UAV) in renewable energy applications has been studied as the design and use of renewable energy infrastructure can be improved. Renewable energy use has increased significantly over the past 10 years, though further improvements are forecast to be both possible and necessary for increased uptake of the technology.

This work aims to determine the most suitable commercial UAV for this task, before investigating the requirements for integrating the range of sensors and mission profiles to outline future upgradability. The UAV selection took place through a market analysis where product specifications were gathered.

The recommended UAV was the Dropbear product from Australian Droid and Robot, which was selected due to its 30 minute flight time, 2 kg payload capacity and low cost. The vehicle can be operated most effectively with the use of a slow acceleration profile, moving to the next waypoint immediately after an image has been captured, using multiple 10 Ah batteries and a recharge station.

Future work includes a detailed analysis of the attachment mechanism for a particular vehicle, before acquiring a vehicle and evaluating its performance to validate the selection methodology.

## 1.0 Introduction

Developments in the fields of Unmanned Aerial Vehicles (UAVs) and renewable energy electricity generation have presented an opportunity for the use of a UAV to improve the maintenance and efficiency of a power plant. In the time between 2000 and 2010, global renewable energy installations more than quadrupled [1], pushed by a need to reduce carbon dioxide emissions. These emissions are predicted to cause future warming and changing precipitation around the world. The International Energy Agency states that in 2012, renewable energy accounted for 12.88% of global energy supply, consequently reducing these emissions.

The Queensland Geothermal Energy Centre of Excellence (QGECE) had applied for a grant to commission a UAV for use in a range of renewable energy applications. Primarily, the UAV is to be used to check the efficiency of mirrors at a future Concentrated Solar Power (CSP) plant located at the University of Queensland (UQ) campus in Gatton, Queensland. The UAV is also to be used to validate simulations of a cooling tower exhaust vent and to make wind resource assessments. The UAV will provide information essential to the efficient operation of these facilities and to improve future designs.

This project aimed to select a commercially available UAV and determine the modifications necessary for the UAV to perform the range of desired applications. The project intended to conclude with a recommendation to the QGECE for the most suitable UAV, as well as the possible configurations of the vehicle and their suitability. The range of applications for which the UAV is to be used will result in contributions to the relevant literature concerning the methodology of UAV selection and modification. The investigation may result in the creation of a new comparison metric, by which vehicles, configurations, and the use of enabling technologies can be efficiently compared.

Rather than designing a new UAV, this project focuses on the modifications required to take a commercially available UAV and implement the system to achieve the desired functions. This has provided the opportunity to minimise the risk associated with the design of a new system, by utilising a system which has already been proven, also minimising the cost associated with the project. The project has not considered the design and selection of sensors, which is the focus of another project, being undertaken by Byron Burgess-Gallop. The integration of the two projects will produce a specification for a UAV equipped with the necessary sensory equipment to meet its requirements.

The project has reviewed literature pertinent to the design of a UAV, and literature relevant to the range of applications being considered, determined the operator capabilities required for the UAV, made recommendations for the selection of a suitable UAV to the QGECE, has defined the integration requirements of each piece of sensory equipment and has created a

new comparison metric to facilitate the selection of a vehicle. It is expected that a UAV can be chosen to meet the required capabilities. Successful completion of the project also requires the availability of sensors which can take the required measurements, while being carried by the UAV.

The project will produce a methodology for the selection of the most suitable commercially available UAV, and a new comparison metric. These deliverables will take the form of a thesis, which has been organised into Sections 2-5.

Section 2 details the background information relevant to the thesis, in the areas of Concentrated Solar Power, Wind Power, Power Plant Cooling Towers and Comparisons between the various forms of renewable energy. This section outlines why the implementation of a UAV is necessary.

Section 3 outlines the literature relevant to Unmanned Aerial Vehicle design, as well as the process of determining user requirements and making a vehicle recommendation. This section determines the vehicle which will best satisfied the presented requirement.

Section 4 discusses the implementation of the recommended vehicle, including the sensory equipment, relevant operational scenarios, relevant enabling technologies and the upgradability of the vehicle.

Section 5 concludes the report by summarising the results and reflecting on how the project performed relative to the initial aims.

## 2.0 Background

### 2.1 Concentrated Solar Power

A renewable technology becoming increasingly popular is Concentrated Solar Power (CSP). A 1 MW CSP installation stops the emission of 1360 tonnes of carbon dioxide, compared to a coal/steam cycle power plant, and a saving of 688 tonnes of carbon dioxide over a combined cycle system [1]. The intermittency inherent to several other types of renewable energy can be overcome with a CSP plant connected to a thermal storage system, at a much greater efficiency than possible for the storage of electricity [1]. This combination of plant and storage decouples the energy collection and electricity production processes, a highly desirable feature [2].

CSP plants can utilise several different technologies, including the most mature and widely implemented parabolic trough systems, as well as tower systems, parabolic dishes and linear Fresnel reflectors. Tower systems typically operate in three stages: solar energy is received from the sun on mirrors, called heliostats, the energy is directed to a central receiver, before a thermodynamic cycle is implemented to generate electricity. A typical surface area for heliostats is between 40 and 120 square metres, with a two-axis tracking system required to focus all mirrors on the receiver [1]. Thermodynamic cycle efficiency increases from a parabolic trough receiver system to a central receiver system, and increases again when moving to a dish receiver with engine [2].

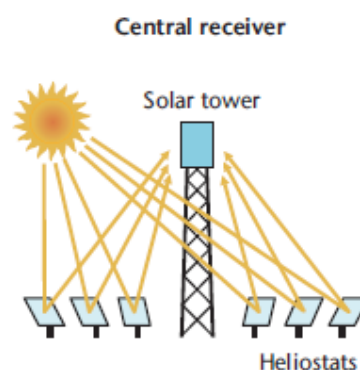


*Figure 1 - Arrangement of components at a CSP Plant [3]*

As the diffuse component of the solar energy can't be optically focused, it is the direct normal irradiance (DNI), or the perpendicular component, which must be exploited at a CSP plant. CSP developers often use a threshold DNI of 1900-2100 kWh per square metre per year for a particular location [1]. It is also important to consider the proportion of the day for which the location receives enough direct sunlight to outweigh the losses of the system. Regions of

optimal DNI are typically found between latitudes of 15° and 40° North or South, in semi-arid or arid areas with reliably clear skies. Lack of clear skies close to the equator in summer, as well as cloudiness and small DNI above 40°, make other latitudes unsuitable.

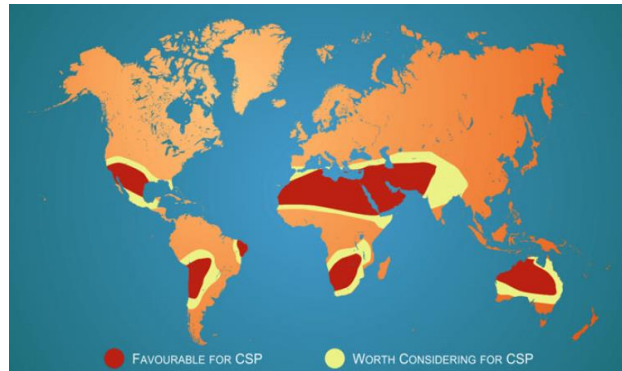


Figure 2 - DNI across the world [1]

Thermal storage can overcome many of the disadvantages of renewable energy systems, though, to be effective, a suitably large solar field would be required [2]. Conversely, a CSP plant would be able to provide baseload power with integrated storage. Considerations for this storage include the selection of materials, operating temperatures, insulation, and required night time duration. Typical storage materials are salts, ideally with high heat retention properties. Rankine, Brayton, Stirling and combined cycles are being used for electricity generation. Another possibility is the Kalina cycle, which utilises a mixture of water and ammonia. Outputs from solar technology are expected to be enhanced by the use of supercritical steam and carbon dioxide cycles, as well as air Brayton cycles.

In Australia in 2015 two large scale solar thermal plants were operational. The contribution of solar thermal to the generation of renewable energy in Australia was only 0.08%. Figure 2 shows that most of Australia has a DNI which is either favourable for CSP or worth considering for CSP, meaning that the contribution of solar thermal could be significantly greater.

Unlike photovoltaic panels, the mirrors used at a CSP plant are significantly affected by the build-up of dirt, due to the mirrors having a much smaller numerical aperture than the panels, and so being greatly affected by the scattering caused by dust and dirt [5]. Effective and efficient methods are required to keep the mirrors operating at maximum efficiency.

Deposited particles could be dust, water stains, carbon from smoke, or pollen from agricultural regions, having differing sizes and shapes [6]. It is also noted that high solar radiation intensity areas, suitable for a CSP plant, are typically dry and windy desert regions. While the wind can sweep dust from the mirrors, this dust and that lifted from the ground, becomes suspended in the air, and eventually resettles on the mirrors. There are a range of regimes which describe the dominant mechanism for scattering of light due to the particles, where  $D$  is the particle diameter,  $n$  is the refractive index and  $\lambda$  is the wavelength of light [6].



Table 1 - Scattering Regimes [6]

Rayleigh theory	$\frac{\pi D n}{\lambda} < 0.6$	Equation 1
Scattering is a reflection	$\frac{\pi D}{\lambda} > 0.6$	Equation 2
Mie theory	$\frac{0.6}{n} < \frac{\pi D}{\lambda} < 0.6$	Equation 3

Diameters of wind driven sand of 60-2000  $\mu\text{m}$ , silt of 4-60  $\mu\text{m}$ , and clay of less than 4  $\mu\text{m}$  [7]. The effect of differing particle sizes is also apparent, that being the ability of small particles to fill the voids between big particles, the effect of which is omitted from the regimes described by Equations 1-3 [7]. By substituting a diameter of 60  $\mu\text{m}$ , and using a visible wavelength of light, into Equations 1, 2, and 3, it is apparent that the condition for Equation 2 is satisfied and the scattering will be a reflection. The extent to which a mirror is contaminated can then be determined by the amount of light which is reflected off the particles, and not a reflection of the mirror.

## 2.2 Wind Power

Wind power is typically generated by horizontal axis three-bladed wind turbines, with the power extracted being proportional to the area covered by the rotating blades, air density and the cube of wind speed. For wind power generating systems to operate effectively, wind speeds of 8-12 m/s are required for extended periods of time. Larger wind speeds can cause damage to the turbine, due to the turbulence which occurs at the blade tips, where the larger radial distance from the hub results in the largest linear speeds [8]. Increasingly the installation of these wind turbines is moving from on-shore to off-shore locations, where the wind is less turbulent and more constant and predictable [1]. In Spain, Portugal and Denmark, wind power already provides 15 to 30% of the generated electricity [9]. This will avoid the emission of 4.8 Gt of carbon dioxide per year.

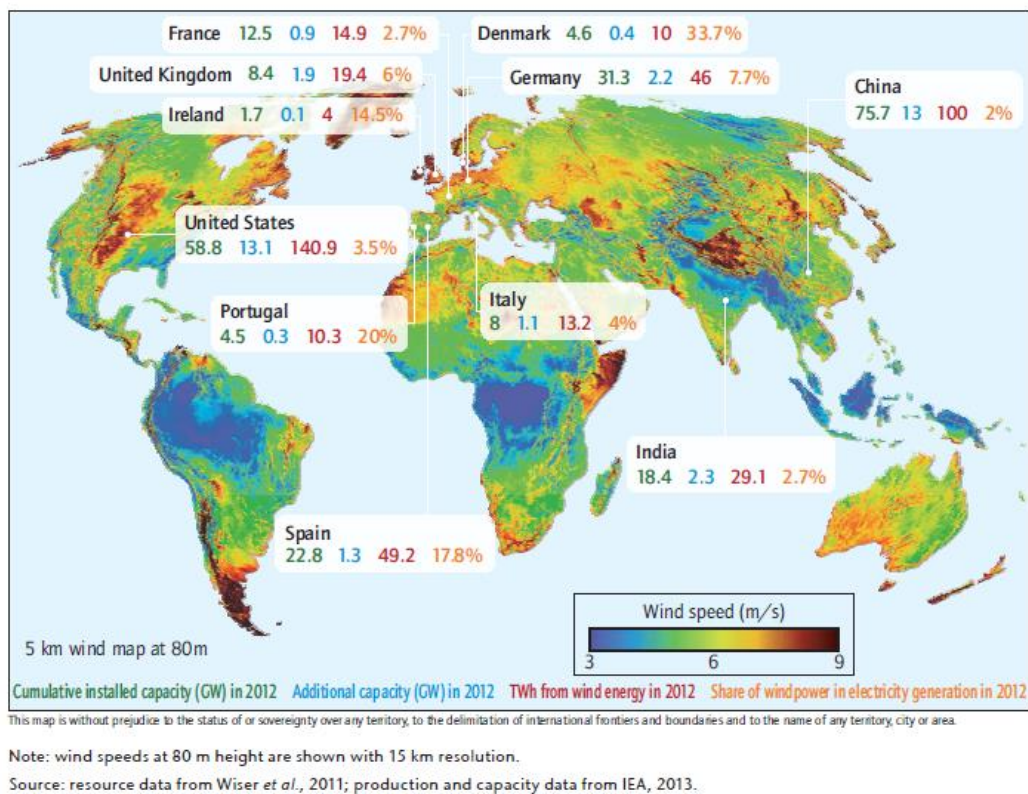


Figure 3 - Availability of Wind Energy across the World [9]

The conversion of wind energy into electricity has a typical maximum efficiency of 40%, due to Betz Law and losses in converting from mechanical power. Betz Law describes the inability of a wind turbine to capture all of the instantaneous wind power, as that would stop the wind and prevent new wind from reaching the turbine.

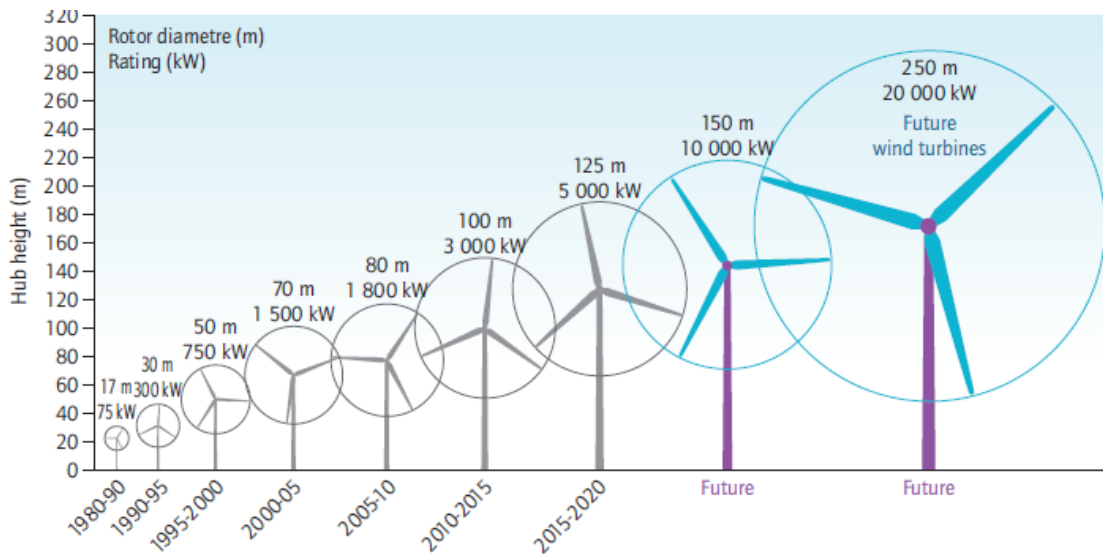


Figure 4 - Increasing Size of Wind Turbine Blades over Time [9]

As the power extracted by a wind turbine is proportional to the area covered by the rotating blades, the maximum diameter of the circle covered by the blades has grown as the technology has been further developed. The maximum diameter is expected to be 150 m in the near future [9]. Correspondingly, the power capture of wind turbines is expected to grow from typically 5 MW up to 10 MW [9]. As rotor diameters increase towards 250 m, it is expected that power generation could reach 20 MW, though it is unclear if the trend of increasing rotor diameter and achieving a corresponding increase in power generation can continue indefinitely.

As of 2015, Australia has combined wind capacity of 4187 MW with 2062 turbines from 76 wind farms [10]. This provides 33.7% of the generated renewable electricity. However, Australia still places 16<sup>th</sup> in the world for installed wind capacity. Referring to Figure 3, much of Australia has wind speeds ideal for the generation of wind power, suggesting that the energy production of wind power could be significantly greater.

Wind energy is characterised by its intermittency and non-manageable behaviour [1]. Hence, the ability to store energy from periods of high production for use when there is little wind would be highly desirable. A noteworthy solution is Compressed Air Energy Storage (CAES), which is initialised by compressing air to a high pressure. The compressed air can then be stored, and is mixed with natural gas and expanded in a combustion gas turbine to regenerate electricity. It is expected that wind energy and CAES will have significant market penetration in future.

Due to the significant capital investment required to construct and commission a wind turbine, precise initial and ongoing wind resource assessments are required. Initially this assists in the selection of the best location for the construction of a wind farm, but continues as a method of predicting the electricity production of the farm.

## 2.3 Power Plant Cooling Towers

The implementation of an electricity generating thermodynamic cycle occurs through a power plant. These thermal power plants produce waste heat as a byproduct, the effectivity of the constant dissipation of which has implications for the efficiency of the whole cycle.

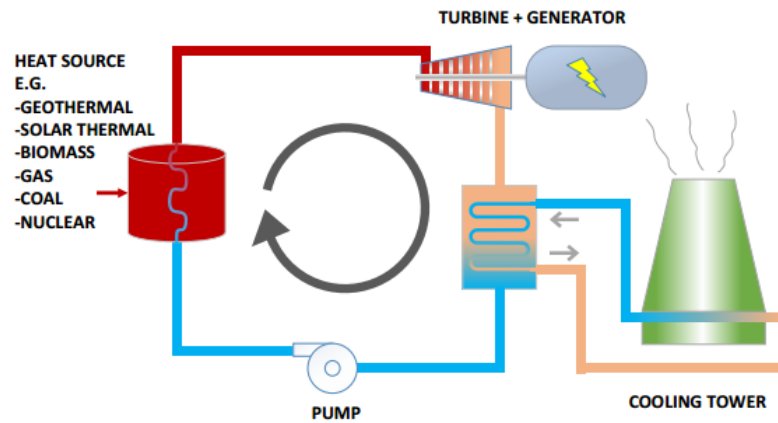


Figure 5 - Schematic of the relevant cycle, showing the cooling tower [11]

Figure 5 illustrates the arrangement of components in a typical power plant. Initially the working fluid acquires energy from the source as heat, before the fluid cools as energy is extracted by the turbine. Before the fluid is sent by the pump back to the source, a cooling tower is used to efficiently dissipate waste heat to the environment.

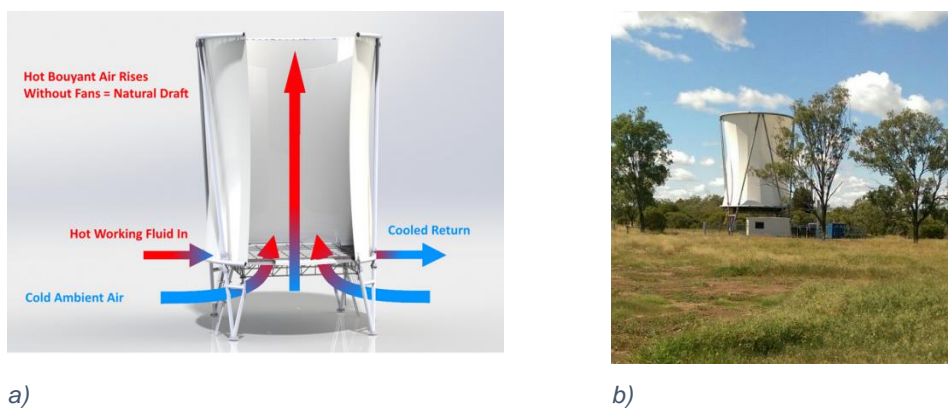


Figure 6 - Cooling tower schematic (a) and photo of the experimental unit (b).

Cooling towers can be classified as being wet, if the evaporation of water into the air flowing through the tower cools the working fluid, or dry, if the working fluid transfers heat straight to the air. The selected mode of operation depends on the availability of water, with the less efficient dry method being the only possible choice if water can't be used, despite the reduced efficiencies at high ambient temperatures. To effectively operate dry, additional heat exchangers are required, presenting a higher initial cost in commissioning the system.

One method of wet tower operation is to inject water at the top of the tower, allowing it to flow downward, against the flow of the air. Fans can be placed at the top or bottom of the cooling tower to assist the effects of buoyancy. It is also common for a packing material to be placed inside the tower, providing a large surface area for the air and water to contact.

Another method of operating the tower is with hybrid cooling. In this technique, water is introduced into the air stream in the inlet. The water droplets evaporate, cooling the air stream, providing a larger temperature differential between the air flow and the working fluid. More generally, the performance of a cooling tower is dependent on the physical design, air and water flows, as well as the ambient wet-bulb temperature, which is the lowest temperature which can be reached with the evaporation of water.

The cooling tower at UQ Gatton utilises a steel frame to support a PVC polymer membrane, which facilitates natural, draft cooling of a bed of heat exchangers at the bottom of the tower. The cooling tower, designed to support remote, small scale power stations in the 1 – 10 MW capacity range, has an easily deployable modular design and is significantly cheaper to construct than a typical concrete cooling tower [11]. The design can also present significant water savings when operated dry, utilising the buoyancy of the warm air within the tower.

Future design improvements for the Gatton cooling tower include the use of solar collectors. These solar collectors heat the air moving through the cooling tower, increasing its buoyancy and causing more air to flow through the tower. Improvements to the cooling tower design can be assisted by the validation of exhaust simulations.

## 2.4 Comparisons

The International Energy Agency aims for 11% of global electricity generation to be from concentrated solar by 2050, 3.5% from geothermal and 15 to 18% from wind, with a total of 75% of generated electricity being derived from renewable sources. It is also noted that concentrated solar, and other renewable energy generation techniques, require large capital investment. Lowering the cost of capital, through research, will increase the uptake of concentrated solar power. In Australia, in 2015, only 14.6% of generated electricity was derived from a renewable source, with 33.7% of that from wind, 0.08% from solar thermal and only a negligible amount from geothermal [10]. 14.6% of generated electricity is approximately equivalent to providing power to 6.7 million homes.

The Large-scale Renewable Energy Target (LRET) in Australia for 2020 was reduced from 41000 GWh to 33000 GWh in 2015. In 2015, only 15200 GWh of large-scale renewable energy was generated. To begin bridging the difference, construction or planning approvals have been given to 8 GW of wind power projects and 2.5 GW of solar power [10].

In markets such as New Zealand and Brazil, on-shore wind power can compete without support in the electricity marketplace [9]. Total investment cost ranged from 900-1400 USD per kW in 2011 for an on-shore turbine. Operation and maintenance costs for wind power plants are very low compared to conventional fuel plants, typically accounting for 2-4% of the total costs of the farm [9].

Geothermal investment costs are highly variable, but can range from 2000-4000 USD per kW for the common flash technology plant [9]. Investment cost for a combined cycle gas power plant are typically around 1000 USD per kW [2]. The price of coal, oil and gas is still lower than renewable sources, indicating that resources still need to be allocated to the renewable field to make the sector competitive.

In Australia, comparisons can be drawn between the methods of generating electricity by using the Levelised Cost of Electricity (LCOE) [12], which captures the lifetime cost of producing electricity from a technology. This allows a comparison between a gas-fired generator, having moderate initial costs with continuing fuel and operational costs, with a solar photovoltaic system, which has a high initial investment cost but very low operating costs [12]. It is important to note that the LCOE does not take into consideration the flexibility, or lack of, a technology to generate additional or decreased amounts of power to match the demand. The metric also doesn't consider how different technologies may play different roles in the electricity system.

In 2015, the LCOE was lowest for natural gas combined cycle and supercritical pulverised coal, with wind being the lowest cost large-scale renewable energy source [12]. Figures 7 and

8 shows the LCOE predictions for 2020 and 2030, with wind power being the most competitive [13].

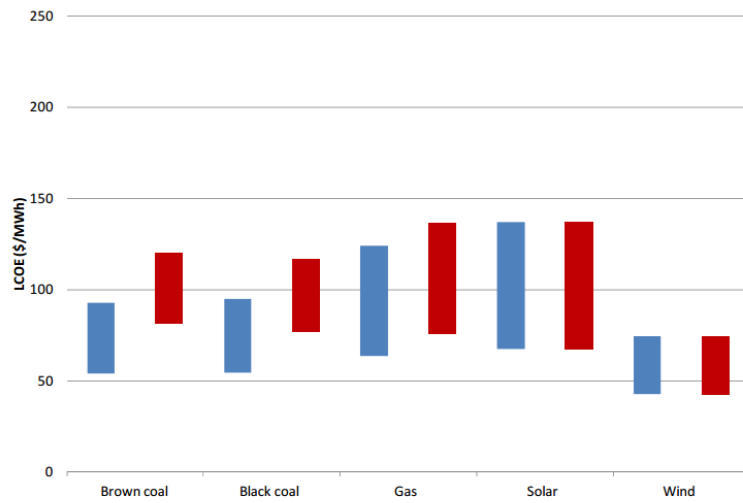


Figure 7 - LCOE Prediction for 2020. Red bars are with the implementation of a carbon price in Australia, while blue bars are without the implementation of a carbon price. [13]

The introduction of a carbon price has a pronounced effect on gas, and brown and black coal. With the carbon price, both the solar and wind renewable options have a smaller LCOE than the coal and gas options. Without the carbon price, both coal options have a comparable LCOE to wind power.

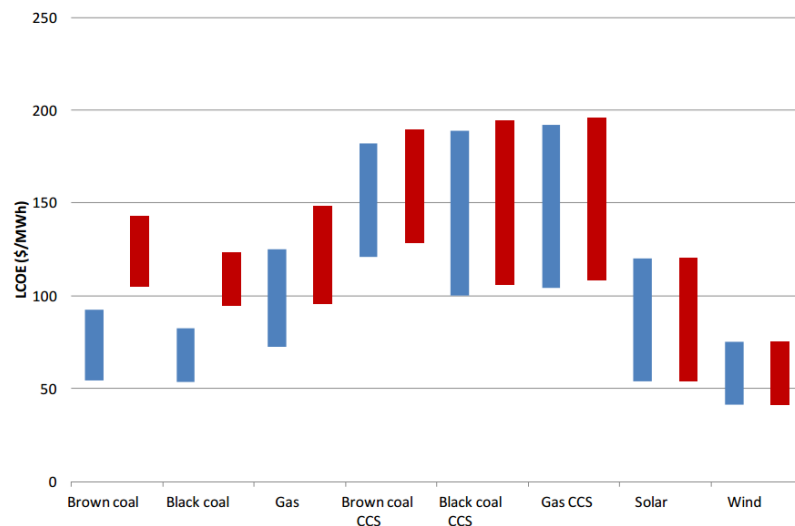


Figure 8 - LCOE Prediction for 2030. Red bars are with the implementation of a carbon price in Australia, while blue bars are without the implementation of a carbon price. The effect of Carbon Capture and Storage (CCS) is also shown. [13]

Comparing Figures 7 and 8 reveals that little difference in price of wind is observed between 2020 and 2030, while projected reductions in the cost of capital are expected to reduce the

cost of solar power. The difference caused by the carbon price has become more pronounced for the non-renewables without CCS.

Figure 8 shows that, for the CCS options, only a small difference exists between the carbon price and non carbon price options. This is due to the carbon price being paid on emissions, which are significantly reduced when a capture and storage methodology is in place. CCS can capture around 90% of emissions [13].

Figures 7 and 8 have been generated using the assumption that significant technological benefits are to be made, meaning that research must continue in these areas for these goals to be achieved.



## 3.0 Unmanned Aerial Vehicle

### 3.1 Unmanned Aerial Vehicle Literature

Unmanned Aerial Vehicles (UAVs) are controllable, aerodynamic lift generating vehicles which function without an on-board operator. They typically comprise of a structure, aerodynamic elements, propulsion mechanisms and a control system [4]. Types of UAVs include the quadcopter and fixed wing designs. The quadcopter consists of a body with several small electric motors, with propellers, which largely provide thrust in a vertical direction, while a fixed wing UAV instead has a fixed lift generating surface with motors to generate thrust in the horizontal direction. These two types have been illustrated in Figure 1.

UAVs can have a variety of sizes, designed to meet the requirements of a particular application. A quadcopter may be able to fly at approximately 50 km/h for 30 minutes, with dimensions less than 0.5 m in each axis. For comparison, the fixed wing Northrop Grumman Global Hawk utilises a turbofan engine to cruise at 575 km/h for a maximum duration of 32 hours, assisted by a 40 m wingspan. The ability to hover and perform Vertical Take-off and Landing (VTOL) makes the quadcopter, and similar designs, more suitable for some applications than the fixed wing type.



a)



b)

Figure 9 - a) ADR Dropbear Quadcopter [10], b) Northrop Grumman Global Hawk Fixed Wing UAV [14]

The development of UAVs has been driven by the possibility of military usage. This can be traced to as early as 1917, with the implementation of the Kettering Aerial Torpedo and the Sperry-Curtis Aerial Torpedo, and has continued to the present day, with UAVs such as the Global Hawk, Figure 1b, and the Predator [4]. UAVs are also being used in applications including for TV and cinema, atmospheric and meteorological research, and for agricultural requirements. In 2006, it was thought future applications would include various monitoring and surveillance tasks, as well as for telecommunications and atmospheric sampling [15].

Motivators of the use of UAVs include cost-effectiveness and the efficiency of missions being improved by moving from manned aircraft to UAVs [15]. It is also noted that the use of UAVs has been hindered by the immaturity of the market, insufficient safety and reliability, and high costs. High acquisition costs result from the low volume of production, with high development costs, while high operational costs result in a high cost of ownership.

Key enabling technologies for the small scale UAV market are Lithium Polymer (LiPo) batteries, MEMS inertial and environmental sensors, GNSS solutions, brushless motors and electronic speed controllers, and suitable microprocessors [16]. The light weight and high power density of LiPo batteries is essential, as is the accelerometers and gyroscopes which comprise the MEMS inertial sensors and the magnetometer and barometer which comprise the environmental sensors. Suitable microprocessors are those which have a high computational ability, but are inexpensive and only require a small amount of power. The flight computers also require a small form-factor, such that they can fit on the vehicle.

Brushless motors, or electronically commutated motors, are motors which function via an integrated switching power supply, and have a higher efficiency and reduced mechanical wear compared to brushed motors. The motors require limits in the software or they can burn out, which occurs when the motor reaches a temperature such that the epoxy resin melts. Full battery voltage signals are converted to throttle orders by the electronic speed controllers. However, these controllers required a calibration for the throttle range [16].

Pertinent design notes for a UAV include the placement of components on the airframe. The flight computer requires adequate cooling, while the MEMS accelerometers should be mounted on vibration isolation mounts. The antenna cable should be kept as short as possible, while the GNSS receiver should not be obstructed, and magnetometers should be kept away from high voltage lines and motors.

High quality aerial photos, taken with a UAV, have been used to create a digital surface model of a geothermal steam field, with sufficiently high resolution to be of comparable quality to LiDAR, at a significantly reduced cost [17]. UAVs have also been used to safely and accurately map physical and biological characteristics of geothermal environments using a thermal infrared camera [18], as well as map heat patterns of cryptic geothermal fumaroles, at altitudes unsafe for manned aircraft [19].

Reconnaissance missions are the vast majority of work undertaken by UAVs, with the stabilised platform of the payload of central importance [4]. This provides the angular stability necessary for many missions. Torsional modes of vibration, involving the rotation of the structure, are typically most easily excited in a UAV, due to the motors. These modes are also the most damaging for stability. A well designed gimbal will work to stabilise these vibrations, and will often include structures with high torsional stiffness, such as closed tubes. The use of

a platform for the payload may allow the design of easily interchangeable payloads to suit a range of applications.

Limited literature exists to show that UAVs have been used at CSP or geothermal power plants. Conversely, for the wind farm case, it is apparent that UAVs have been employed extensively. Work includes preliminary surveying of sites for wind farms [20], estimating the average annual energy production by collecting data for the wind resource distribution [21], as well as using a number of UAVs to measure wind and perform 3D photogrammetry [22].

Work performed by UAVs includes tasks which are often considered to be dull, dirty and dangerous. However, a range of innovations are still in development. The danger that someone will be harmed by a rotating propeller exists whenever a person is near a flying UAV. Solutions for this include having a concentric frame rotate around the propellers, which, when encountering an increased level of resistance, will generate the electromagnetic field necessary to electromotively brake the propeller, avoiding injury [23]. Alternate quadcopter configurations are also being investigated, including the central placement of one large motor and propeller and having the remaining three motors equally spaced around the perimeter. The single large propeller presents significant efficiency improvements, while manoeuvrability is still achieved by the three small motors [23].

In applications where the UAV must travel from a starting location to the desired position, where it will be flying around, but doesn't have an inherent need to be airborne during the transit, it is possible to capitalise on ground effects. The effect of being near the ground, within approximately two rotor radii, is to create a spring-like cushion of air. The cushion increases the lift generated by the rotors as the dispersion of the wake from the rotors is limited. It is also possible for ground effects to be recognised by the flight control system, such that increased precision can be achieved for landings [23].

UAV flight in Australia is governed by Civil Aviation Safety Regulation (CASR) 1998 Part 101, which provides direction for the safe and legal operation of UAV systems [24]. Section 7.1.1 notes that no restrictions are placed on the operation of a small UAV, provided that the UAV is not operated above 400 feet above ground level, and remains clear of designated airspace, aerodromes and populous areas. This will be the regime of flight for the CSP and geothermal plant operations, but may not be the case for the wind farm application, which may require the UAV to fly in excess of 400 feet above ground level. In this regime, the UAV must be flown in accordance with any conditions imposed by the Civil Aviation Safety Authority (CASA), which may include specifying maximum altitudes and particular times the UAV is permitted to fly.

### 3.2 Selection Criteria and Considered Vehicles

The recommendation of a suitable UAV to the QGECE has been based on the identification of a range of capabilities which are required from the system. Table 1 outlines the capabilities that are required from the system, which the proposed UAV, after modification, will meet.

Table 2 – Capabilities of the System Introduced by the Modifications

<b>Capability</b>	<b>Description</b>
C1	The system shall determine whether a mirror requires cleaning
C2	The system shall make the determination for every mirror
C3	The system shall visit every mirror
C4	The system shall precisely determine its distance from an object
C5	The system shall store all recorded measurements
C6	The system shall measure wind speed and direction
C7	The system shall record wind speed and direction parameters in several locations around a wind turbine
C8	The system shall be able to take uninterrupted measurements for at least 30 minutes
C9	The system shall measure temperature and humidity
C10	The system shall record temperature and humidity parameters in the exhaust of a cooling tower

Several capabilities shown in Table 1 also fall within the scope of the project undertaken by Byron Burgess-Gallop, which concerns the design and selection of a range of sensors and measurement equipment. Table 2 details the capabilities which are out of scope of this project, as these are capabilities which will be required in the supplied UAV.

Table 3 – Capabilities of the System Prior to Modification

<b>Capability</b>	<b>Description</b>
C11	The system shall transmit its location to the base station
C12	The system shall return to the starting position if battery levels reach a critical level
C13	The system shall return to the starting position if the route is blocked
C14	The system shall return to the starting position if a mirror can't be found
C15	The system shall return to the starting position if other errors occur

A market analysis has been performed to select the commercially available UAV which has the capabilities described in Table 3 and facilitating those shown in Table 2. The analysis was conducted with several criteria to be considered, including price, payload capacity, range, speed, flight duration, having a GPS autopilot and being equipped with a stabilised gimbal. Appendix A shows the complete list of considered systems.

A total of 24 UAV systems, from 12 manufacturers, were considered in the market analysis, encompassing a range of recreational and commercial systems, as well as considering quadcopters, hexacopters, octocopters, and helicopters. Pricing estimates varied significantly for the considered options, ranging from approximately \$500 to \$100000 AUD. The fixed wing UAV design would be unsuitable for each of the intended applications, as it will be necessary to hover in each case. It was found that every system, except the ATI AGHeli, was equipped with a stabilised gimbal. The AGHeli, a small petrol engine helicopter, designed for the spraying of agricultural fields, would not require the ability to do this.

Material selection was not a differentiator between the products, with carbon fibre widely used across the range of considered products. As there was no requirement for the mass of the vehicle itself, this was not a primary criteria, however, may have been a deciding factor between two otherwise very similar UAVs, with the lighter vehicle requiring less power to remain in flight than the heavier option. Similarly for the range and maximum speed, these were not as critical as the flight duration, being able to fly for at least 30 minutes. While the UAV will require a payload capacity, this capacity can be quite small, thanks to the light sensors to be utilised

The ability to enter GPS waypoints for a flight was found to be only provided by a small number of systems. The systems eliminated at this stage included the leisure style UAVs, designed with line of sight operation intended. While many of those systems provided the necessary flight time and duration, at a price minimised by the large volumes of production, it is essential for the intended system that the UAV is able to travel autonomously. This left products from Aeronavics, Aibotix, Australian Droid and Robot, HSE and Microdrones. HSE products were deemed unsuitable due to their significant purchase prices, while pricing information could not be found for the Microdrones products.

The Aeronavics Skyjib and Aibotix Aibot X6 both provide the required payload capacity, as well as the stabilised gimbal and GPS waypoint capabilities, but are unable to fly for a duration of 30 minutes, not being able to satisfy C8. An additional factor to consider is the proximity of the manufacturing location to Brisbane, Queensland, which may facilitate quick maintenance to minimise downtime. While the X6 are not constructed in Brisbane, Aibotix do have a representative present who could facilitate contact with their head office. The Aeronavics Navi was found to be more expensive than the ADR Dropbear, and Aeronavics do not have a supplier in Brisbane, and instead delivering and supporting from New Zealand.

### 3.3 Recommendation

This report recommends the selection of the Australian Droid and Robot Dropbear quadcopter, which proved competitive in each of the selection criteria, and is constructed locally in Brisbane, Queensland. This system has a 2.0 kg payload capacity, 30 minute flight duration, is equipped with a stabilised gimbal and includes a payload mounting system.

The Dropbear motor and propeller combination has been sourced from T-motor, with MN5208 850 W motors paired with 16×5.4 carbon fibre blades. The motors draw power from the 22.2 V LiPo 10 Ah battery. The battery also powers the Futaba T8J 2.4 GHz remote control system, 3DR Pixhawk autopilot, 3DR GPS units, 915 MHz telemetry system, and 6S power distribution unit.



*Figure 10 - ADR Dropbear.*

A ready to fly mass of 3.8 kg means that with a payload of 2 kg, the maximum takeoff mass would be 5.8 kg. The carbon fibre frame is able to be folded, to assist with storage, as well as facilitating transport in a Pelican hardcase. The vehicle is assembled, calibrated and tested by ADR before delivery.

## 4.0 Implementation of the Vehicle

### 4.1 Sensors

Critical to the successful implementation of the vehicle is the integration of the sensors. Each of the pieces of measurement equipment has requirements which must be satisfied for the equipment to properly capture data. As noted in the Introduction, this project is closely linked to another project, which was to select the most suitable sensors to complete the aims of the vehicle. This section will outline the requirements of each of the selected sensors, shown in Appendix B.

Global Positioning System (GPS) sensors are used to determine position by triangulating with satellites. The selected sensors are from Adafruit and have a precision of 1.8 m and 0.1 m/s. Section 4.3 will detail an enabling system which can improve this level of precision. The sensors require 100 mW of power, have a mass of 8.5 g, and a price of \$60.31. The sensor has a small footprint of 25.5 mm by 35 mm by 6.5 mm, as well as having two mounting holes.

Inertial Measurement Unit (IMU) determines the orientation of the vehicle with the use of an accelerometer, gyroscope and magnetometer. The selected sensors are from Adafruit, have a power requirement of 20.8 mW, a mass of 2.8 g and a price of \$44.34. The sensor has a small footprint of 38 mm by 23 mm by 3 mm, as well as having four mounting holes.

These GPS and IMU sensors are in addition to those which come pre-installed on the ADR Dropbear vehicle, and are required to take measurements independent of those required by the UAV control system, such that the information can be used by the other sensory equipment.

Ultrasonic distance sensors are used to determine the distance between the vehicle and another object. This occurs with the sensor sending out an ultrasonic wave and receiving the wave back once it has been reflected off another object. These sensors have a range of up to 5 m and a precision of 3 mm. An ultrasonic distance sensor is required on each of the front, back and bottom surfaces of the vehicle, to ensure the vehicle remains clear of obstacles and equipment. The total power requirement is then 225 mW, with a mass of 25.5 g at a price of \$15.03. The sensor has four mounting points.

The temperature and humidity sensor provides the temperature and humidity. This shouldn't be biased by the temperature or moisture output of components of the vehicle. This sensor has a power requirement of 7.5 mW, a mass of 2.5 g, and a price of \$13.18. The sensor has a single mounting hole.

The pressure sensor provides the pressure. This sensor is required for determining the flow properties in the exhaust of the cooling tower. The sensor requires 1 mW of power, has a negligible mass and a price of \$5.99. This sensor has a small footprint of 3.6 mm by 3.8 mm by 0.93 mm.

The image sensor captures an image such that it can be processed to determine whether a mirror requires cleaning. The selected sensor for this is the GoPro camera, which has an 8 MP sensor. The GoPro requires 2000 mW of power, has a mass of 74 g and a price of \$299.95. The camera dominates the power, mass and cost requirements of all the sensors. This requires an unobstructed view of the mirror to be checked. The camera would also need to be mounted on a stabilised gimbal to minimise the noise present in images.

The wind sensors have been selected to provide wind speed and direction information. These are required for both the wind power and cooling tower applications. The sensors must not be skewed by the effect of air being drawn into or pushed away from the propellers. The mechanism by which this could be performed is yet to be confirmed.

For the complete set of sensors, the total power requirement is 2354.3 mW, with a mass of 113.3 g, and a price of \$438.80. The power requirement corresponds to 1.1% of the capacity of the 22.2 V, 10 Ah battery, so its effect will be marginal. The maximum payload of the Dropbear is 2 kg, so this is less than 6% of the capacity, when all the sensors are installed. The price of \$438.80, compared to the \$5000 cost of the vehicle, corresponds to a 9% increase in the cost of the system.



## 4.2 Operational Scenario

The implementation of the operational concept begins with the user installing the relevant module of sensors on the UAV. The user then enters the list of GPS waypoints which the UAV is to visit, before the UAV takes off and travels to the first waypoint. At each waypoint, the UAV will pause for a period, determined by the application, to record the relevant measurements. The UAV will then return to the starting point once all the waypoints have been visited, or when the flight control system detects a low battery level or other mission ending condition.

For the concentrated solar power application, the UAV captures an image at each waypoint and transmits this to the base station while moving to the next mirror. While in transit and as the UAV captures an image of the following mirror, the ground station processes the image, instructing the UAV to return to the previous mirror to capture another image if a determination can't be made from the original image. Hence, if another image must be taken, the UAV won't have travelled any further away than the next mirror, reducing the time spent back tracking. Figure 11 shows this sequence in a flow chart.

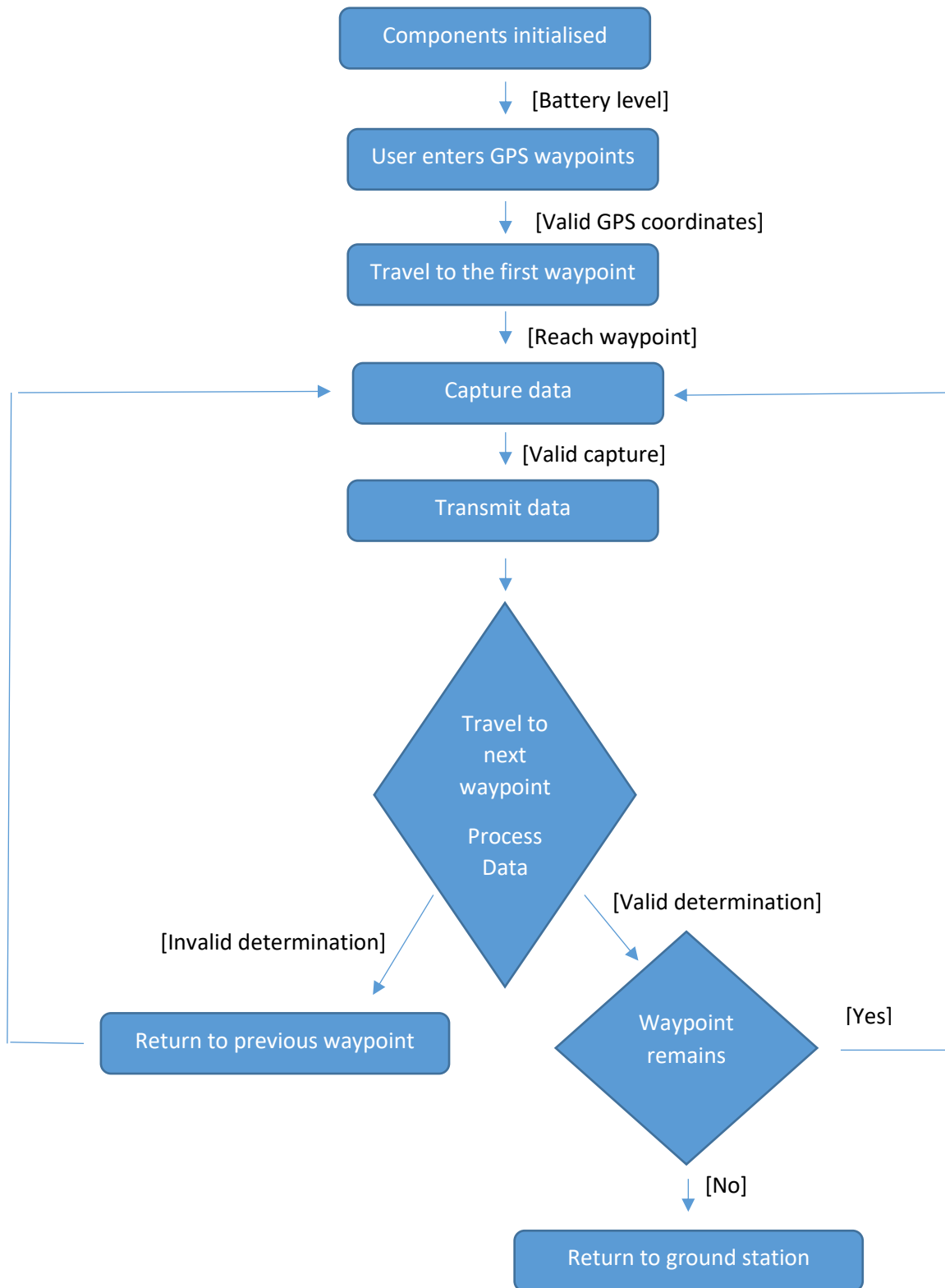


Figure 11 - Operational scenario flowchart

It is apparent that an optimisation problem exists whereby the UAV should follow the path through each of the points which provides the shortest travel time. A brute force optimisation is unfeasible in this instance as the problem has a solution space of  $\frac{(n-1)!}{2}$  for  $n$  nodes. This is the classic “Travelling Salesman” problem, for which solutions exist in literature, including the concept of Simulated Annealing. This methodology is derived from the physical process of heating a metal to a high temperature and slowly cooling it, initially allowing atoms with sufficient energy to diffuse across short distances, before changes to the material cease once the metal has finished cooling. In the Simulated Annealing algorithm, random movements through the domain are permitted at early time steps, when the metal would still be hot. As time progresses, movements through the domain become more selectively allowed, such that only better solutions are permitted.

### 4.3 Enabling Technologies

In systems engineering, the design process differentiates between the system of interest and any other relevant systems, systems which enable the system of interest to function in the desired manner.

Section 4.1 noted that the GPS sensors have a precision of 1.8 m. Whether or not this is acceptable is dependent on the application, with a higher level of precision required to locate each of the mirrors. A possible solution is the use of a real-time kinematic GPS sensor [25], which could provide an uncertainty of 0.5 m. This connects two individual receivers via a dedicated serial data link. Each receiver computes its location, before exchanging information to cancel common errors and reduce noise to more precisely determine the locations. The receivers exchange pseudorange, carrier phase and Doppler measurements via the data link.

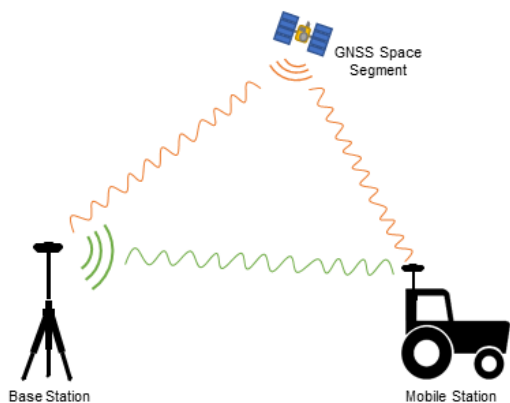


Figure 12 - Real time kinematics system [26]

Figure 12 shows how the GPS receiver on the mobile station receives signal from the satellite, as well as receiving a signal from a base station of known location.

The continuous operation of the vehicle throughout the night would require some combination of batteries and charging equipment. For the ADR Dropbear, battery packs of both 10 Ah and 6.6 Ah were available. One solution to this problem has been proposed, whereby the vehicle returns to a ground station and swaps batteries, allowing the vehicle to continue operating, while the depleted battery is recharged in preparation for a future battery swap [27]. The simultaneous changing and charging of batteries then allows the UAV to operate indefinitely, provided a sufficient number of batteries exist to ensure that at least one has been recharged by the time the UAV has depleted each of the other batteries.

The solution proposed in [27] addresses requirements that the system be portable, that the system would be required to interface with small and delicate batteries, that the system would be required to provide power to the UAV while the battery change occurs, and to minimise the

downtime of the UAV. The problem of vehicles being underutilised is noted for systems which only have the ability to charge the battery, as the vehicle is grounded for the recharge time. Several charging methods were also considered, including a copper contact system, an inductive and capacitive power transfer, and using high energy lasers, though the change-charge system was found to provide the best vehicle utilisation.

The design of the change-charge system, shown in Figure 13, consists of a dual rotating drum structure, to queue the batteries while they are charged.

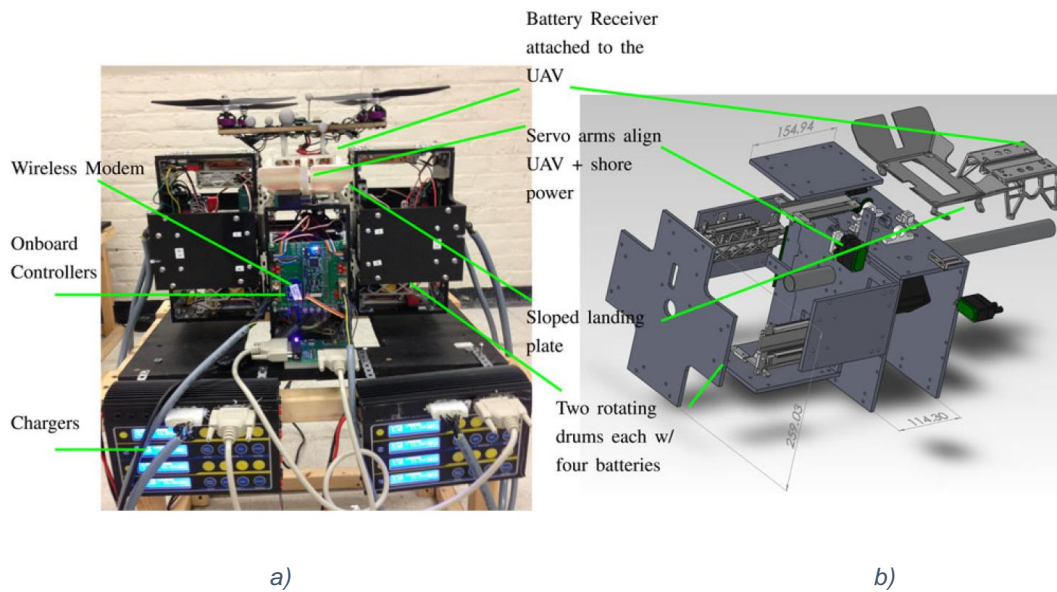


Figure 13 - Battery recharge station. Experimental unit (a) and CAD drawing (b) of the left drum, for simplicity [27].

## 4.4 Upgradability

A number of factors influence the operation of the vehicle, including the battery size, operational requirement and usage.

$$10 Ah = z A \times 0.5 \text{ hours}$$

$$z = 20 A$$

Discharge at 20 A to provide the listed 30 minutes of endurance.

$$4 \times 543.8 W = 22.2 V \times Y$$

$$Y = \frac{4 \times 543.8 W}{22.2 V} = 98.0 A$$

The maximum safe continuous discharge rate can be calculated to determine if this is safe.

$$10C = 10 \times 10 Ah = 100 A$$

As  $98 A < 100 A$ , this discharge rate is safe. The endurance of the vehicle at this discharge rate can also be calculated.

$$\frac{10 Ah}{98 A} = 0.1 \text{ hours} = 6 \text{ minutes}$$

Hence, at the maximum rate of safe continuous discharge, the battery will be drained in approximately 6 minutes.

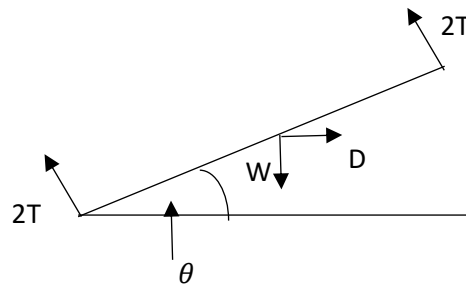


Figure 14 - Free Body Diagram

Figure 14 shows the free body diagram, for the vehicle and its propulsion mechanism.

In the vertical direction,

$$4T \cos \theta = W$$

The thrust can then be calculated by assuming an angle of  $25^\circ$ .

$$T = \frac{mg}{4 \cos \theta} = \frac{3.8 \times 9.81}{4 \times \cos 25} = 10.3 N$$

This corresponds to a kilogram force of 1.0 kg from each motor, in order to keep the vehicle level.

In the horizontal direction,

$$a = \frac{F}{m} = \frac{\eta 4T \sin \theta}{m} = \frac{0.7 \times 4 \times 4 \times 3.273 \times 9.81 \times \sin 25}{3.8}$$

$$= 40.0 \frac{m}{s^2}$$

Hence the maximum acceleration possible from the vehicle is 40 m/s<sup>2</sup>.

It has been assumed that the average distance between mirrors at a CSP plant is 20 m. Each of the velocity profiles has been generated such that a distance of 20 m is covered.

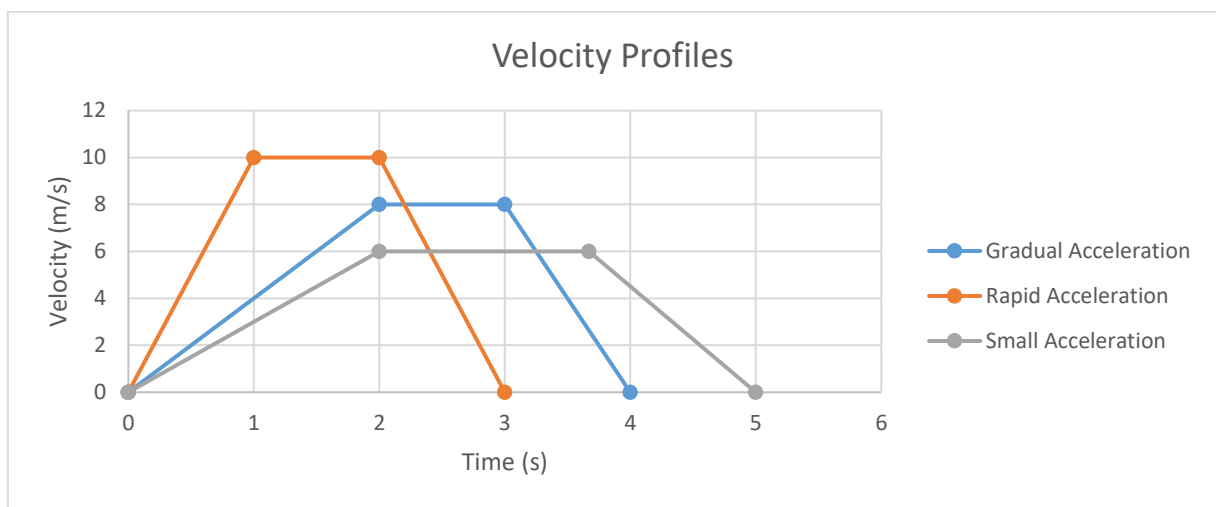


Figure 15 - Rapid, gradual and slow acceleration profiles, each covering a distance of 20 m.

For the constant velocity portion,

$$distance = velocity \times time$$

For the acceleration portions,

$$distance = \frac{acceleration \times time^2}{2}$$

For each of the acceleration profiles, the corresponding motor performance must be determined. The Dropbear is fitted with four T-motor MN5208, with the relationship between thrust and power as given by Figure 16.

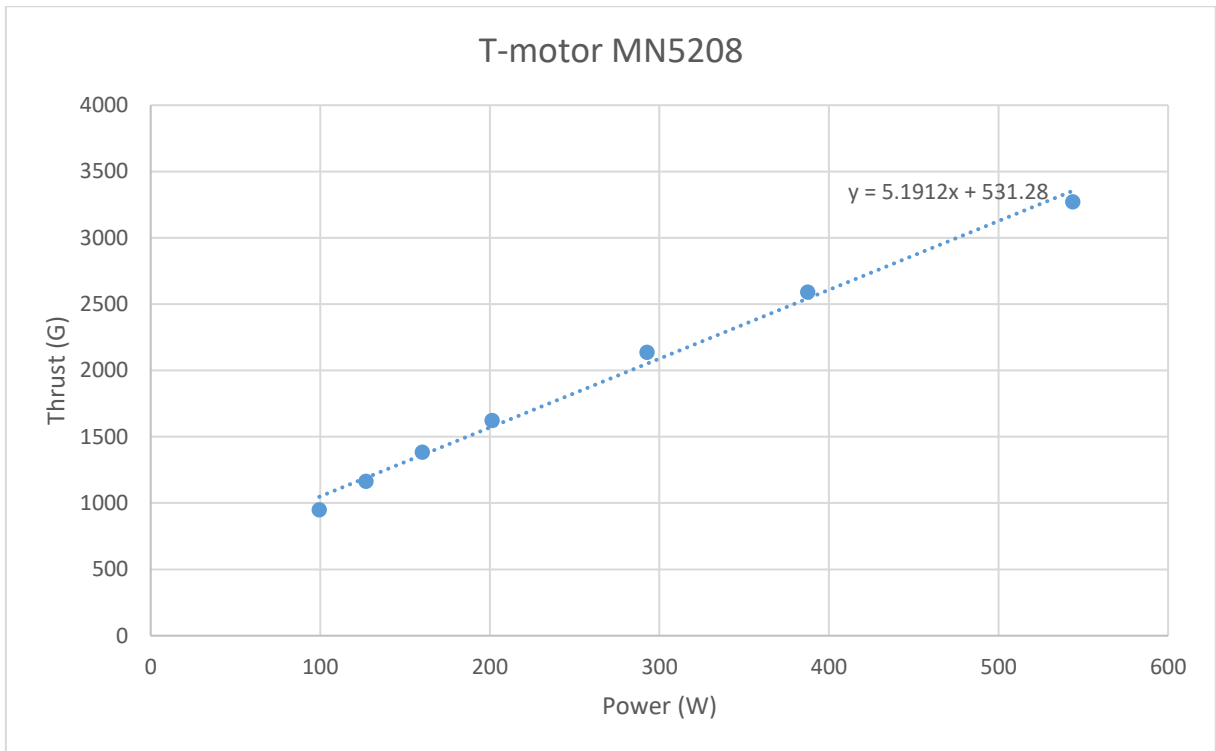


Figure 16 - Thrust and power draw information for the T-motor MN5208 and 16\*5.4 propeller combination.

$$x = \frac{y - 531.28}{5.1912}$$

$$T = \frac{ma}{4\eta \sin \theta} = \frac{3.8 \times a}{4 \times 0.7 \times \sin 25}$$

Table 4 - Average power consumption for each acceleration profile based on power consumption of each phase of the flight.

	Acceleration	Constant velocity	Deceleration	Hover	Average power consumption
Rapid	$T = 32.1 N$ $P = 528.2 W$ $t = 1 \text{ second}$	$P = 99.4 W$ $t = 1 \text{ second}$	$T = 32.1 N$ $P = 528.2 W$ $t = 1 \text{ second}$	$P = 99.4 W$ $t = 5 \text{ seconds}$	$P = 206.6 W$
Gradual	$T = 12.9 N$ $P = 149.9 W$ $t = 2 \text{ seconds}$	$P = 99.4 W$ $t = 1 \text{ second}$	$T = 12.9 N$ $P = 149.9 W$ $t = 1 \text{ second}$	$P = 99.4 W$ $t = 5 \text{ seconds}$	$P = 116.2 W$
Small	$T = 9.6 N$ $P = 86.8 W$ $t = 2 \text{ seconds}$	$P = 99.4 W$ $t = 1.67 \text{ seconds}$	$T = 9.6 N$ $P = 86.8 W$ $t = 1.33 \text{ seconds}$	$P = 99.4 W$ $t = 5 \text{ seconds}$	$P = 95.2 W$



For the rapid acceleration profile,

$$\frac{4 \times 206.6 \text{ W}}{22.2 \text{ V}} = 37.2 \text{ A}$$

$$\frac{10 \text{ Ah}}{37.2 \text{ A}} = 0.27 \text{ hours} = 16 \text{ minutes}$$

Subtract a minute to allow for time moving between the mirrors and the recharge station.

$$\frac{15 \text{ minutes} \times 60 \text{ seconds per minute}}{8 \text{ seconds per measurement}} = 112 \text{ measurements}$$

For the gradual acceleration profile,

$$\frac{4 \times 116.2 \text{ W}}{22.2 \text{ V}} = 20.9 \text{ A}$$

$$\frac{10 \text{ Ah}}{20.9 \text{ A}} = 0.48 \text{ hours} = 29 \text{ minutes}$$

Subtract a minute to allow for time moving between the mirrors and the recharge station.

$$\frac{28 \text{ minutes} \times 60 \text{ seconds per minute}}{9 \text{ seconds per measurement}} = 186 \text{ measurements}$$

For the slow acceleration profile,

$$\frac{4 \times 95.2 \text{ W}}{22.2 \text{ V}} = 17.2 \text{ A}$$

$$\frac{10 \text{ Ah}}{17.2 \text{ A}} = 0.58 \text{ hours} = 35 \text{ minutes}$$

Subtract a minute to allow for time moving between the mirrors and the recharge station.

$$\frac{34 \text{ minutes} \times 60 \text{ seconds per minute}}{10 \text{ seconds per measurement}} = 204 \text{ measurements}$$

Hence, 112 measurements can be achieved for the rapid acceleration profile, 186 from the gradual acceleration profile and 204 from the slow acceleration profile per battery. However, this information alone does not provide sufficient information to determine which option is best, as the 112 measurements are completed in 16 minutes while the 204 measurements require 35 minutes. The effect of the velocity profiles on the number of measurements which can be completed in a single night, roughly 8 hours, is shown in Figure 17.

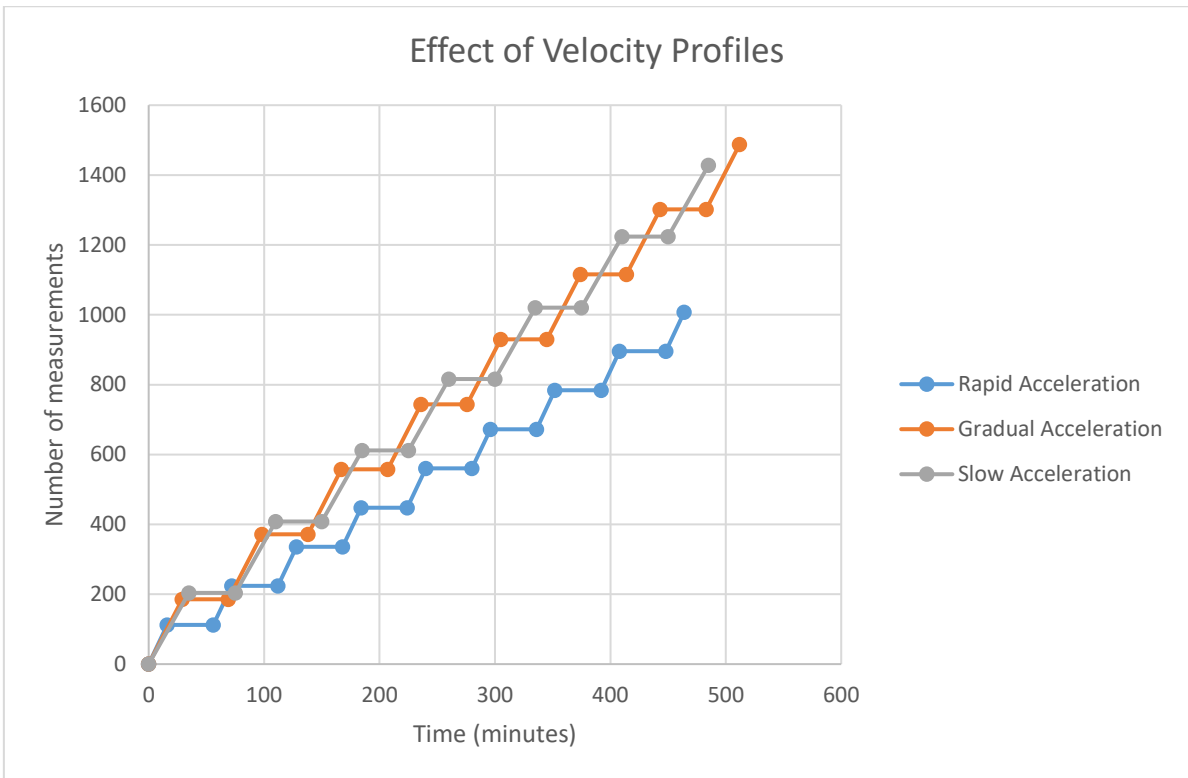


Figure 17 - Effect of the velocity profile on the number of mirrors which can be assessed each night.

The image is sent to the ground station for processing, which takes 10 seconds including the time taken for transmission. After processing, the ground station can determine whether an image is suitable to determine whether the mirror requires cleaning, and can instruct the UAV to return to the mirror and capture another image if necessary.

Considerations for the previous calculations include the efficiency between the battery and motors, as well as the change in capacity of the battery with the discharge rate.

As outlined in Section 4.2, the camera will not have a 100% success rate, and the ground station is able to instruct the UAV to return to a mirror if it has continued. To evaluate this, several success rates have been considered to determine at what observed success rate it is more efficient to wait than move on. In the wait scenario, the UAV captures an image, transmits the image and hovers until the image has been processed. If the image is then valid, the vehicle moves to the next mirror, whereas if the image is not valid then the UAV will capture and transmit another image before again waiting to ensure the image is valid. In the return scenario, the UAV captures and transmits an image before immediately moving to the next mirror. Only if the image is processed and considered to be invalid will the vehicle return to the previous mirror.

Table 5 shows the average time to take a measurement for each success rate and scenario. In every case, it is advantageous to move to the next mirror and then only return to the previous mirror if necessary.

Table 5 - Success rate and average time based on two operational sequences.

Success rate (%)	5	10	25	50	75	90	95
Average return time (seconds)	24.25	23.5	21.25	17.5	13.75	11.5	10.75
Average wait time (seconds)	34.25	33.5	31.25	27.5	23.75	21.5	20.75

Two battery options have been considered, the Multistar 10000 mAh and 6600 mAh batteries. The 10000 mAh battery has a constant discharge rate of 10C.

The 10000 mAh battery has an endurance of 30 minutes. Allowing a minute to move to and return from the mirrors, it can then be assumed that

$$\text{Number} = 28 \text{ minutes} \times 4 \text{ mirrors per minute} = 112 \text{ mirrors}$$

The 6600 mAh battery has an endurance of 20 minutes. Allowing a minute to move to and another minute to return from the mirrors, it can then be assumed that

$$\text{Number} = 18 \text{ minutes} \times 4 \text{ mirrors per minute} = 72 \text{ mirrors}$$

The recharge time of each battery has been calculated by assuming a recharge at a voltage of twice the amperage of the battery [28], that is, for a 10 Ah battery a recharge amperage of 20 A can be used. A recharge calculator [29] has then been used to determine the battery recharge time, with this being 40 minutes for each battery. This allows for a 40% efficiency loss.

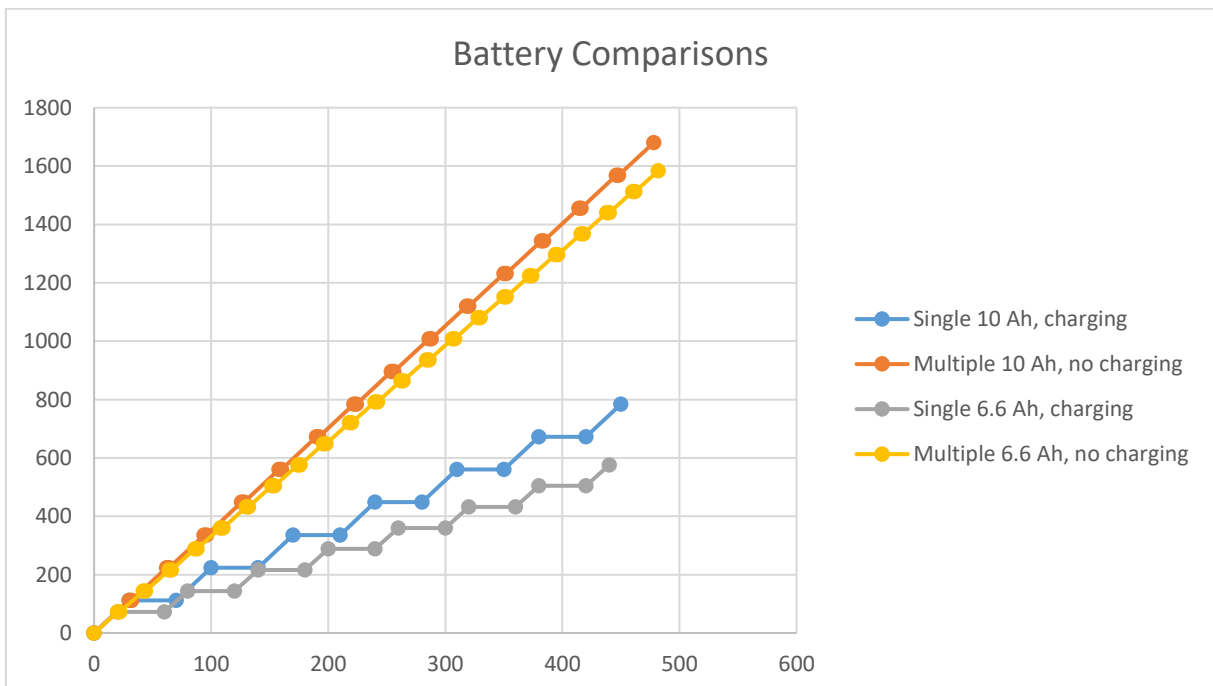


Figure 18 - Battery capacity comparison.

$$\text{Comparison metric} = \frac{\text{Number of mirrors surveyed per night}}{\text{Cost of specific required equipment}}$$

To generate this metric, the cost of the specific required equipment has been summarised in Table 6. The completion of Table 6 will become part of future work.

*Table 6 - Contribution of specific equipment to the overall cost.*

Equipment	Cost
Real time kinematics	
Battery recharge station	
Additional batteries	
Sensors	438.80

## 5.0 Conclusion

Unmanned Aerial Vehicles (UAVs) have been used in a variety of applications. Several different types of UAV exist, including the quadcopter. Previous work with UAVs has included research to create high resolution digital surface models, mapping characteristics of an area, and using a thermal infrared camera to map heat patterns. Limited literature exists to show that UAVs have been used at CSP or geothermal power plants. Conversely, for the wind farm case, it is apparent that UAVs have been employed extensively.

Tower systems typically operate in three stages: solar energy is received from the sun on mirrors, called heliostats, the energy is directed to a central receiver, before a thermodynamic cycle is implemented to generate electricity. Unlike photovoltaic panels, the mirrors used at a CSP plant are significantly affected by the build-up of dirt. The extent to which a mirror is contaminated can then be determined by the amount of light which is reflected off the particles, and not a reflection of the mirror.

In a thermodynamic cycle, a cooling tower is used to efficiently dissipate waste heat to the environment. The cooling tower at UQ Gatton utilises a steel frame to support a PVC polymer membrane, which facilitates natural, draft cooling of a bed of heat exchangers at the bottom of the tower. Improvements to the cooling tower design can be assisted by the validation of exhaust simulations.

Wind power is typically generated by horizontal axis three-bladed wind turbines, with the power extracted being proportional to the area covered by the rotating blades, air density and the cube of wind speed. Due to the significant capital investment required to construct and commission a wind turbine, precise initial and ongoing wind resource assessments are required.

The recommended UAV was the Dropbear product from Australian Droid and Robot, which was selected due to its 30 minute flight time, 2 kg payload capacity and low cost. The vehicle can be operated most effectively with the use of a slow acceleration profile, moving to the next waypoint immediately after an image has been captured, using multiple 10 Ah batteries and a recharge station.

Future work includes a detailed analysis of the attachment mechanism for a particular vehicle, before acquiring a vehicle and evaluating its performance to validate the selection methodology.

## 6.0 References

- [1] Guerrero-Lemus, R & Martinez-Duart, JM 2013, *Renewable Energies and CO2*, Springer-Verlag, London.

The textbook contains a good description of the general CSP plant function, types of CSP technologies, locations where CSP technology is suitable, thermal storage, financial considerations, improvements in the optical technology to reduce the number of times the mirrors need to be washed as well as the amount of water needed for each wash. Also mentioned are the development of cleaning robots. This was similar in nature to the work of this project, however, these robots don't make a determination regarding whether a mirror requires cleaning, and instead every mirror is cleaned. This was a well reference text which provided a great deal of useful, background information.

- [2] Veeraragavan, A 2016, *Solar Energy*, Powerpoint slides, University of Queensland, Brisbane

The presentation has been prepared for delivery in an Energy Systems course at UQ, providing an overview of both photovoltaic and solar thermal styles of solar energy capture. For each technology, the author provides an overview of the physical principles which underline the technology. The continued use of graphs and figures makes the presentation approachable for someone with little previous knowledge.

- [3] International Energy Agency, *Technology Roadmap Solar Thermal Electricity*, 2014

The International Energy Agency has presented an updated report on the current state of solar thermal electricity technology and uptake, with the hope of informing policy-makers and businesses on how to implement strategies to increase the usage of the technology. The report is correspondingly limited in its ability to demonstrate state of the art technologies by technical rigour, though this could be considered a strength for appealing to the general reader.

- [4] Fahlstrom P & Gleason, T 2012, *Introduction to UAV Systems*, Wiley, 4<sup>th</sup> edition.

Fahlstrom and Gleason take the opportunity in this work to clarify the general understanding of the typical reader as to the nature and breadth of Unmanned Aerial Vehicle systems. The tone of the work makes it enjoyable to read, with explanations largely given in a qualitative sense. Quantitative analysis is also utilised effectively. A strength of the text was the presentation of historical information regarding the first vehicle which could be referred to as a UAV by the current definition. While now approaching 4 years since publication, this text was relatively recent, which proved very valuable for gauging the current state of UAV technologies.

- [5] Presentation and Discussion with Paul Meredith, Director of UQ Solar

This was an informal session in which the Director largely spoke about the implementation of the photovoltaic solar field at UQ Gatton. The has proven to be very valuable, contextualising the technology within the electricity grid and marketplace, and providing insights into the economic considerations of the technology. While largely providing background information, this source was particularly relevant regarding the importance of the numerical aperture of a mirror, and how dust has an adverse effect on the energy capture.

- [6] Ghazi, S, Sayigh, A, Ip, K 2014, Dust effect on flat surfaces – A review paper, *Renewable and Sustainable Energy Reviews*, 33, 742 - 751

The article provides a thorough overview of the effect of dust on photovoltaic panels. The results of a number of studies are presented, highlighting the effects of different locations, impurities and cleaning mechanisms. The authors conclude that the effect of deposited particles and dust on photovoltaic panels is complex, varying with climate, environment and location, and that the most appropriate cleaning method will depend on these factors. The authors have presented information from a number of sources, highlighting the differing results obtained from those. While the article has a particular focus on photovoltaics, not the focus of this project, the presentation of the Rayleigh and Mie theories of scattering proved to be useful.

- [7] Beattie, N, Moir, R, Chacko, C, Buffoni, G, Roberts S, Pearsall, N 2012, Understanding the effect of sand and dust accumulation on photovoltaic modules, *Renewable Energy*, 48, 448-452

The experimentation was conducted by using a sieve to filter the deposition of particles on the photovoltaic panel surface. The results were also compared with numerical simulations. The article highlights how experimental results are often presented but that the physical origins of the effect were not investigated or understood. The article goes some way to correct this deficiency by building an exponential decay model from first principles, as well as including a discussion of the effects of clustering. The article has been limited by the studying of only one type of particle, meaning that the effect of small particles filling the voids provided around big particles has not been considered. While the article focused on work related to photovoltaic panels, the work broadly relates to this research.

- [8] Taylor D (2004) *Wind energy* (Chap. 7). *Renewable energy*. Oxford University Press, Oxford

The source provides a good overview of several aspects of wind energy, and was used to verify the information provided by other sources. Particularly noteworthy was the discussion surrounding the maximum speed of a rotor, which is limited by the effects of turbulence at the tip of the blades. The source was limited by the early

publication date, which means developments of the last decade have not been covered.

[9] International Energy Agency 2013 Technology Roadmap Wind energy

The International Energy Agency has presented an updated report on the current state of wind energy technology and uptake, with the hope of informing policy-makers and businesses on how to implement strategies to increase the usage of the technology. The report is correspondingly limited in its ability to demonstrate state of the art technologies by technical rigour, though this could be considered a strength for appealing to the general reader.

[10] Clean Energy Council, Clean Energy Australia Report 2015,

The Clean Energy Council has prepared this report to detail the current uptake of various types of renewable energy, as well as the targets which are set for the future and how they can be met. This source was particularly useful for moving from a global focus to a focus on the renewable energy situation in Australia. A strength of the report is the way abstract figures have been turned into an equivalent number of homes to be powered, for example, making the report tractable to a non-technical audience.

[11] Gwynn-Jones, S, Atrens, A, Guan, Z, Lu, Y, Russell, H, Gurgenci, H, Hooman, K, Queensland Geothermal Energy Centre of Excellence, Hybrid Natural Draft Dry Cooling Towers – An Enabling Technology for Remote Area Thermal Power Generation in Australia, University of Queensland

This paper outlines the background material and reasons for the construction of the cooling tower at UQ Gatton, as well as how it will be utilised in research, and how the technology is to be implemented in small, regional towns. A strength of the paper was the way the need for an efficient and cost effective small cooling tower was the focus, leading to clear and direct benefits.

[12] Graham, P 2016, Wind, solar, coal and gas to reach similar costs by 2030: report, The Conversation

This article presented the results of the CSIRO study in an accessible way, such that they could be easily understood. This was a good summary, which could have been strengthened by the selection of figures which more effectively illustrated the messages which were being written about.

[13] Brinsmead, T, Hayward, J & Graham, P 2014, Australian electricity market analysis report to 2020 and 2030, CSIRO Report No. EP141067

The report provided projections of various energy generation technologies and their market penetration at the current and in future times. The models used to generate these projections were clearly outlined, making the report very transparent. Also



included were figures which provided a clear visual indication of the meaning and relationship between results.

- [14] NASA, NASA Armstrong Fact Sheet: Global Hawk High-altitude, long endurance science aircraft, accessed on 14 May 2016, <<http://www.nasa.gov/centers/armstrong/news/FactSheets/FS-098-DFRC.html>>.

The website outlines a range of facts and figures of the Northrop Grumman Global Hawk, a fixed wing UAV. It is noted that the aircraft used for high-altitude, long range missions, a domain inaccessible to a quadcopter. This information, and photos, were useful to illustrate the fixed wing UAV concept.

- [15] UVS 2006 International Presentation

The presentation provides guidance on how to classify a variety of unmanned aerial vehicles, and their uses. Despite now being 10 years post publication, the source was useful for evaluating how the predictions made at the time have eventuated, largely being valid. A strength of the presentation would be the listing of advantages and disadvantages of various technologies, permitting an easy comparison between them.

- [16] Creagh, M 2016, Unmanned Aerial Vehicles and Electric Propulsion, Lecture Slides, The University of Queensland, Brisbane

This lecture provided an introductory level understanding of unmanned aerial vehicles and electric propulsion, which was easily accessible to someone without any prior knowledge. This lecture could have been improved by providing references to further reading for those readers who want their knowledge further extended.

- [17] Harvey, M, Pearson, S, Alexander, K, Rowland, J & White, P 2014, Unmanned Aerial Vehicles for Cost Effective Aerial Orthophotos and Digital Surface Models, University of Auckland, New Zealand

The research details how high quality aerial photos, taken with a UAV, have been used to create a digital surface model of a geothermal steam field, with sufficiently high resolution to be of comparable quality to LiDAR, at a significantly reduced cost. This was particularly useful for understanding the use of UAVs in similar work.

- [18] Nishar, A, Richards, S, Breen, D, Robertson, J, & Breen, B 2015, Thermal infrared imaging of geothermal environments and by an unmanned aerial vehicle (UAV): A case study of the Wairakei-Tauhara geothermal field, Taupo, New Zealand

UAVs have been used in this research to safely and accurately map physical and biological characteristics of geothermal environments using a thermal infrared camera. This research is noteworthy for demonstrating the feasibility of implementing a UAV and camera system, but it has reduced applicability to this research as the focus of the investigation was the geothermal environment.

- [19] Nishar, A, Richards, S, Breen, D, Roberston, J, & Breen, B 2016, Thermal infrared imaging of geothermal environments by UAV (unmanned aerial vehicle), NRC Research Press

Apparently following their earlier work (2015), the research details the investigation of and mapping of heat patterns of cryptic geothermal fumaroles, at altitudes unsafe for manned aircraft. The research was limited by a lack of discussion surrounding the use of the UAV, and a lack of schematics or diagrams to engage the reader.

- [20] Manyoky, M, Wissen Hayek, U, Klein, T, Pieren, R, Heutschi, K, & Gret-Regamey, A, Concept for Collaborative Design of Wind Farms Facilitated by an Interactive GIS-based Visual-acoustic 3D Simulation

The work focuses on the preliminary surveying of sites for wind farms, facilitated by a UAV. This work is consistent with the bulk of work currently being undertaken with UAVs, using them for mapping and surveillance. As for many other works, the investigation does not primarily focus on the particulars of the UAV, rather the use of the wind farm, also important for this research.

- [21] Grassi, S, Chokani, N & Abhari, R 2012, Large Scale Technical and Economical Assessment of Wind Energy Potential with a GIS tool: Case study Iowa

The authors have demonstrated how an estimate can be made for the average annual energy production by collecting data for the wind resource distribution. Using the case study for the state of Iowa in the United States of America, this demonstrates the expanse of area which can be covered and evaluated with a UAV.

- [22] Jensen, A, Morgan, D, Chen, Y, Clemens, S & Hardy, T 2009, Using Multiple Open-Source Low-Cost Unmanned Aerial Vehicles (UAV) for 3D Photogrammetry and Distributed Wind Measurement, ASME International Design Engineering Technical Conference

This research, utilising a group of fixed wing UAVs, notes how to measure wind and perform 3D photogrammetry by making use of the number of measurement locations. The work had limited applicability to this report, but did demonstrate the capturing of data related to making a wind resource assessment, which is essential to the effective selection of a location for a wind farm.

- [23] Davis, E & Pounds, P 2016, Passive Position Control of a Quadrotor with Ground Effect Interaction, IEEE Robotics and Automation Letters, Volume 1

Pounds and Davis have provided a very well written article regarding the details of a quadrotor which is subject to ground effects. The paper begins with a strong introduction, highlighting the need for this technology, and setting the tone for what continues to be a thoroughly well explained and detailed publication.

- [24] Civil Aviation Safety Authority, Civil Aviation Safety Regulation 1998 Part 101

The Australian Civil Aviation Safety Authority has produced this document to clarify the requirements for safe and legal operation of an unmanned aerial vehicle. The document was very useful for determining the altitudes above ground level at which the vehicle can operate without restriction, and the procedure for when operation is expected to be beyond these regimes.

- [25] Montenbruck, O, Ebinuma, T, Lightsey, G & Leung S 2002, A real-time kinematic GPS sensor for spacecraft relative navigation, Aerospace Science and Technology.

This paper provided an explanation of the initial vision for the use of the real time kinematic technology. This paper provided details sufficient to see how the technology was used in this particular application, but did not provide sufficient information such that the creative thinker could abstract the idea to be applied in another area.

- [26] <http://www.fsd.mw.tum.de/research/sensors-data-fusion-and-navigation/research-and-competence-areas/satellite-navigation/#RealTimeKinematic>

This website outlined details of the real time kinematic technology and its use. The writing regarding the technology was not as strong as other publications, but was greatly assisted by the inclusion of a clear figure.

- [27] Ure, N, Chowdhary, G, Toksoz, T, How, J, Vavrina, M & Vian, J 2015, An Automated Battery Management System to Enable Persistent Missions with Multiple Aerial Vehicles, IEEE/ASME Transactions on Mechatronics, Volume 20

This article provided a thorough and comprehensive review of the general use of unmanned aerial vehicles and their usefulness. Also addressed were the issues regarding the recharging of these vehicles, with the numerous methodologies for this covered. The authors also provided a thorough outline of the reasoning for each feature of their design, and presented validation test results.

- [28] Cobox, Basic understanding of LiPo, Li-ion and LiFePo4 battery, its use and care, accessed 23 October 2016, <<http://www.cobox-ebikes.com/296/basic-understanding-of-lipo-li-ion-and-lifepo4.html>>.

This website provided an introductory level understanding of the terminology of batteries and their meanings. While LiPo battery information was most relevant, the discussion of other battery technologies provided a good understanding of the context from which the LiPo battery technology has emerged as the most popular.

- [29] Battery Charge Time Calculator, accessed 23 October 2016, <<http://www.csgnetwork.com/batterychgcalc.html>>.

This tool proved useful for determining the recharge rates. Particularly insightful was the discussion regarding the efficiencies and their effects on the recharge.

# Appendices

## Appendix A

UAV Name	Type	Price (AUD)	Airframe Material	Mass (kg)	Payload (kg)	Range (km)	Max Speed (km/h)	Max Fit Duration (mins)	GPS Autopilot Capability?	Stabilised Gimbal?
3DR Solo	Quadcopter	1253	-	-	-	-	-	20	No	Yes
Aeronavics Navi	Quadcopter	20000	-	3.8	1.2	-	90	35	Yes	Yes
Aeronavics Skylib	Octocopter	35000	Carbon fibre	11	5	-	70	15	Yes	Yes
Aibotix Aibot X6	Hexacopter	45000-70000	Carbon fibre reinforced polymer	3.4	2	-	50	20	Yes	Yes
ADR Dropbear	Quadcopter	5000	Carbon fibre	3.8	2	-	-	30	Yes	Yes
ATI AGHeli	Helicopter	-	Aluminium and carbon fibre	7.25	-	265	88	180	-	-
ATI AgBot	Quadcopter	-	Carbon fibre	4.7	-	26	61	26	-	Yes
ATI Thor X4	Octocopter	24000	Carbon fibre	15.5	-	-	107	15	-	Yes
DJI Matrice 600	Hexacopter	6400	-	9.6	6	5	64	40	-	Yes
DJI Phantom 4	Quadcopter	2000	Magnesium	1.38	-	5	72	28	-	Yes
DJI Inspire 1	Quadcopter	4000	Carbon fibre	2.935	-	-	79	18	-	Yes
DJI Spreading Wings S900	Hexacopter	2000	Carbon fibre	3.3	4.9	-	-	18	-	Yes
DJI Spreading Wings S1000+	Octocopter	2700	Carbon fibre	4.4	9.5	-	-	15	-	Yes
Draganflyer Commander	Quadcopter	-	Carbon fibre	2.75	1	-	50	45	-	Yes
HongKong GL Industrial	Hexacopter	-	Aluminium	-	3.5	5	54	60	-	Yes
HSE Avenger	Helicopter	104000	-	-	4.5	-	-	45	Yes	Yes
HSE RDASS Q1000	Quadcopter	23000	-	-	0.07	1.6	-	-	Yes	Yes
Microdrones MD4-200	Quadcopter	-	NR Carbon fibre	0.8	0.25	6	28	30	Yes	Yes
Microdrones MD4-1000	Quadcopter	-	NR Carbon fibre	2.65	1.2	20	43	90	Yes	Yes
Microdrones MD4-3000	Quadcopter	-	NR Carbon fibre	10.4	3	50	57	45	Yes	Yes
Walkera QR X350 Pro	Quadcopter	470	-	0.986	0.364	-	-	25	-	Yes
Walkera QR X900	Hex or Quad	6100	-	6.95	-	-	-	14	-	Yes
Walkera Tali H500	Hexacopter	1400	-	2.02	0.48	-	-	25	-	Yes
Yuneec Typhoon H	Hexacopter	1800	-	1.53	-	1.6	36	25	No	Yes

Stabilised Gimbal?	Other Comments	Source
Yes	Recreational product	<a href="https://3dr.com/solo-drone/">https://3dr.com/solo-drone/</a>
Yes		<a href="http://aeronavics.com/fleet/navi-3/">http://aeronavics.com/fleet/navi-3/</a>
Yes	GPS waypoint flight, quick release gear mount for interchange	<a href="http://aeronavics.com/fleet/aeronavics-skylib/">http://aeronavics.com/fleet/aeronavics-skylib/</a>
Yes	Automatic waypoint flight	<a href="https://www.aibotix.com/en/overview-aibot-uav.html">https://www.aibotix.com/en/overview-aibot-uav.html</a>
Yes	Preferred UAV	ADR PDF
-	26 cc Petrol engine	<a href="http://store.aerialtechnology.com/product/ati-agheli-2/">http://store.aerialtechnology.com/product/ati-agheli-2/</a>
Yes		<a href="http://store.aerialtechnology.com/product/agbot-2/">http://store.aerialtechnology.com/product/agbot-2/</a>
Yes		<a href="http://store.aerialtechnology.com/product/thor-x4-ati-octocopter-3/">http://store.aerialtechnology.com/product/thor-x4-ati-octocopter-3/</a>
Yes		<a href="http://www.dji.com/product/matrice600/info#specs">http://www.dji.com/product/matrice600/info#specs</a>
Yes	All DJI Products: UAV needs to visit the waypoints to set them	<a href="http://www.dji.com/product/phantom-4">http://www.dji.com/product/phantom-4</a>
Yes		<a href="http://www.dji.com/product/inspire-1">http://www.dji.com/product/inspire-1</a>
Yes		<a href="http://www.dji.com/product/spreading-wings-s900/info#specs">http://www.dji.com/product/spreading-wings-s900/info#specs</a>
Yes		<a href="http://www.dji.com/product/spreading-wings-s1000-plus">http://www.dji.com/product/spreading-wings-s1000-plus</a>
Yes		<a href="http://www.draganfly.com/uav-helicopter/draganflyer-commander/index.php">http://www.draganfly.com/uav-helicopter/draganflyer-commander/index.php</a>
Yes	Navigation works through Google Maps?	<a href="http://www.uav1.com/sell-3739380-police-uav-drone-hexacopter-google-map-navigation-autopilot-5km-flight-and-video-distance.html">http://www.uav1.com/sell-3739380-police-uav-drone-hexacopter-google-map-navigation-autopilot-5km-flight-and-video-distance.html</a>
Yes	Set GPS waypoints	<a href="http://www.hse-uav.com/avenger_specs.htm">http://www.hse-uav.com/avenger_specs.htm</a>
Yes	Optional Ground Station mode with GPS waypoints	<a href="http://www.hse-uav.com/rdass_1000_4_rotor_electric_uas.htm">http://www.hse-uav.com/rdass_1000_4_rotor_electric_uas.htm</a>
Yes	Microdrones' GPS waypoint navigation software	<a href="https://www.microdrones.com/en/products/md4-200/technical-data/">https://www.microdrones.com/en/products/md4-200/technical-data/</a>
Yes	Microdrones' GPS waypoint navigation software	<a href="https://www.microdrones.com/en/products/md4-1000/at-a-glance/">https://www.microdrones.com/en/products/md4-1000/at-a-glance/</a>
Yes	Microdrones' GPS waypoint navigation software	<a href="https://www.microdrones.com/en/products/md4-3000/technical-data/">https://www.microdrones.com/en/products/md4-3000/technical-data/</a>
Yes		<a href="http://en.walkera.com/index.php/Goods/canshu/id/20.html">http://en.walkera.com/index.php/Goods/canshu/id/20.html</a>
Yes		<a href="http://www.walkera.com/index.php/Goods/info/id/22.html">http://www.walkera.com/index.php/Goods/info/id/22.html</a>
Yes		<a href="http://www.walkera.com/index.php/Goods/info/id/23.html">http://www.walkera.com/index.php/Goods/info/id/23.html</a>
Yes		<a href="http://www.yuneec.com/Typhoon-H">http://www.yuneec.com/Typhoon-H</a>

# Appendix B

Application	Direct Property	Indirect Property	Sensor / Module	Mounting	Manufacturer	Part #	Range	Accuracy	Resolution	Update Rate [Hz]		
General	Real Time	Zenith & Azimuth of Sun Ground Speed Vector	Global Positioning System (GPS)	Internal	Adafruit	ADA746	-	-	1 s	-		
	Latitude, Longitude, Altitude						-	1.8 m 0.1 m/s	0.1 m 0.1 m/s	10		
	Orientation (3-axis)		Distance from Reflector/Tower/Turbine		Inertial Measurement Unit (IMU) - Gyroscope, Magnetometer, Accelerometer	Adafruit	ADA1604	± 250/500/2000 dps	± 10/15/75 dps	16-bit	95/190/380/760	
	Magnetic Field (3-axis)							± 130/810 uT	0.8 uT	16-bit	7.5	
	Acceleration (3-axis)				± 2/4/8/16 g	±20 mg	16-bit	50				
	Vertical Clearance				Ultrasonic Sensor	Downwards	-	018-DB-HC-SR04	2 - 500 cm	3 mm	-	-
	Front Clearance				Ultrasonic Sensor	Forwards						
Back Clearance	Ultrasonic Sensor	Backwards										
Solar Thermal	RBG Image	Reflectance	GoPro Session	Downwards	GoPro	-	400 - 1600 ISO	-	8 MP	10 Hz		
Geothermal	Pressure	Altitude	Barometer	Near Freestream	BOSCH	BMP180	300 - 1100 hPa	± 0.06/0.02 hPa	0.01 hPa	-		
	Temperature	-	Temperature and				-	018-DHT22	-40 - 80 °C	± 0.5 °C	0.1 °C	1 Hz
	Humidity	-	Relative Humidity Sensor		-	0 - 100 %RH	± 2 %RH	0.1 %RH				
Geothermal & Wind	Relative Airspeed Vector & Wind Speed Vector	Absolute Airspeed Vector & Wind Speed Vector	Ultrasonic Windspeed Sensor	Near Freestream								
<b>Total</b>												

Update Rate [Hz]	Power [mW]	Mass [g]	Price [AUD]	Notes	Supplier	Source
-	100.0	8.5	\$60.31	CR1220 Coin Cell Required (15x15x4 mm)	Core Electronics	<a href="http://core-electronics.com.au/adafruit-ultimate-gps-breakout-66-channel-w-10-hz-updates-version-3.html">http://core-electronics.com.au/adafruit-ultimate-gps-breakout-66-channel-w-10-hz-updates-version-3.html</a>
10				uFL Antenna Compatible (38x23x3 mm)		
95/190/380/760	18.3	2.8	\$44.34	(38x23x3 mm)	Core Electronics	<a href="http://core-electronics.com.au/adafruit-10-dof-imu-breakout-13gd20h-ism303-bmp180.html">http://core-electronics.com.au/adafruit-10-dof-imu-breakout-13gd20h-ism303-bmp180.html</a>
7.5	2.5			-		
50	-			-		
-	75	8.5	\$5.01	10 us Trigger Input 15° Measuring Angle	Core Electronics	<a href="http://core-electronics.com.au/hc-sr04-ultrasonic-module-distance-measuring-sensor.html">http://core-electronics.com.au/hc-sr04-ultrasonic-module-distance-measuring-sensor.html</a>
	75	8.5	\$5.01			
	75	8.5	\$5.01			
10 Hz	2000	74	\$299.95			
-	-	-	-			
-	1	-	\$5.99	Included in IMU Module ADA1604 (3.8x3.6x0.93 mm)	Core Electronics	<a href="http://core-electronics.com.au/gy-68-bmp180-digital-pressure-sensor-module-replaces-bmp085.html">http://core-electronics.com.au/gy-68-bmp180-digital-pressure-sensor-module-replaces-bmp085.html</a>
1 Hz	7.5	2.5	\$13.18	-	Core Electronics	<a href="http://core-electronics.com.au/dht22-temperature-and-relative-humidity-sensor-module.html">http://core-electronics.com.au/dht22-temperature-and-relative-humidity-sensor-module.html</a>
<b>Total</b>	<b>2354.3</b>	<b>113.3</b>	<b>\$438.80</b>			